

Specific Rain Attenuation Derived from a Gaussian Mixture Model for Rainfall Drop Size Distribution

K'ufre-Mfon E. Ekerete¹, Francis H. Hunt^{1(✉)}, Judith L. Jeffery², and Ifiok E. Otung¹

¹ Mobile and Satellite Communications Research Group,
University of South Wales, Pontypridd CF37 1DL, UK

{kufre-mfon.ekerete, francis.hunt, ifiok.otung}@southwales.ac.uk

² STFC Rutherford Appleton Laboratory, Harwell Oxford, Didcot OX11 0QX, UK
judith.jeffery@stfc.ac.uk

Abstract. Precipitation, particularly rain affects the millimetre and sub-millimetre frequencies more severely than it does for lower frequencies in the Earth-space path. There is therefore a need for accurate models that will enable the rainfall drop size distribution (DSD) to be better predicted for better planning and improved service delivery. Using data captured at Chilbolton Observatory, this paper looks at modelling the DSD using the Gaussian Mixture Model (GMM), and attempts to predict the specific attenuation due to rain based on this model and compares the result with other well-established statistical models (lognormal and gamma). Results show that specific attenuation tends to increase with the drop sizes, and the smaller drops contribute little to the overall attenuation experienced by signals. Specific attenuation was computed based on several standard statistical distributions, and compared with that derived from the ITU recommendation.

Keywords: Theoretical modelling · Space and satellite communications · Estimation and forecasting · Probability distributions · Rainfall drop size distribution (DSD) · Gaussian Mixture Model (GMM) · Specific attenuation

1 Introduction

Modernity requires vast exchange of information, mostly digital. Information service providers constantly seek new ways and methods to transmit these information efficiently and reliably. In the search for the better transmission of these information, the lower frequency bands are congested, and providers now seek to transmit information using increasingly higher frequencies, where more data can be transmitted more economically.

In the higher frequencies, precipitation, particularly rain plays a great role in the dispersion of transmitted signals, causing attenuation in the received signals. Signals are scattered by raindrops since the transmitted wavelengths are much smaller than the raindrop sizes. There have been several studies [1–3] showing how signals are affected by different sizes of raindrops, and a thorough understanding of the distribution of these

raindrops enables the systems designer to design mitigation plans to ensure a better quality of service delivery.

Kumar *et al.* [1] discusses the effect of ignoring the smaller drop bin sizes, and reaches the conclusion that since the smaller drops contributes little to the overall DSD, hence the attenuation and the removal of the smaller-sized bins have little impact on attenuation. Thurai *et al.* [2] suggests that even with the more sophisticated 2D Video Disdrometer, the readings of the smaller drops are still not good enough to be considered reliable, as it under-estimates the drop densities. Åsen and Gibbins [3] while suggesting that the disdrometer is not sensitive to small drop diameters, and thus mis-estimates the attenuation, goes on to suggest that the difference between measured and modelled attenuation may be due to wind drafts.

Rainfall data collected from the disdrometer located at the Chilbolton Observatory, is analysed and the rainfall drop size distribution (DSD) is determined. The data sometimes suggests the presence of underlying multimodal distribution [4–7]. As well as standard statistical distributions like the lognormal and gamma, the Gaussian Mixture Model (GMM) is used to model the rainfall data.

This work attempts to compute the specific attenuation based on the ITU P R 838 model, and compares the specific attenuation derived from the GMM as well as the other statistical models aforementioned. Section 2 discusses the statistical modelling of rainfall DSDs, looking at the commonly used statistical models for the derivation of the DSDs, and introduces the Gaussian Mixture Model (GMM) as a solution to model multimodal distributions encountered in the data. Section 3 discusses specific attenuation – how the ITU recommendation derives specific attenuation for a given rain rate, as well the derivation of specific attenuation from the distributions by integrating the DSD and the extinction cross section of the drops over the entire bin. Section 4 deals with the data collection and procedures, giving insight into the experimentation and the analyses carried out. Section 5 presents and discusses the results, with Sect. 6 concluding the report.

2 Rainfall DSDs

2.1 Statistical Modelling of DSDs

The rainfall DSD, $N(D)$ is taken as the number of raindrops per unit volume per unit diameter centered on D the drop diameter (in mm), measured in $\text{m}^{-3} \text{mm}^{-1}$, where $N(D) dD$, (in m^{-3}), is the number of such drops per unit volume having diameters in the infinitesimal range $(D - dD/2, D + dD/2)$ [7]. The DSD is significant in the computation of rain rates and signal attenuation. The DSD may vary significantly, yet result in the same rain rate given that a large number of small drops may yield the same rain volume (rain rate) as a small number of large drops. And this may explain why two different DSDs with the same rain rate may give two different attenuation values.

Given that D is a continuous and non-negative, various statistical distributions have been used to model $N(D)$. Marshall and Palmer [8] suggested that DSD is distributed exponentially, and can be represented as

$$N(D) = N_0 \exp(-\Lambda D), 0 < D \leq D_{max} \tag{1}$$

and

$$\Lambda = \alpha R^\beta \tag{2}$$

with D_{max} being the biggest drop diameter measured, where N_0 and Λ (in mm^{-1}) are the intercept and slope parameters respectively, and Λ is dependent on the rainfall rate R (in mm/h). This relationship is however valid for $D < 1.5 \text{ mm}$ [8].

Other studies [9–12] modelled the DSD using the lognormal distribution, given as

$$N(D) = \frac{N_T}{\sqrt{2\pi}\sigma_g(D - \theta)} \exp \left[-\frac{(\ln(D - \theta) - \mu_g)^2}{2\sigma_g^2} \right] \tag{3}$$

with σ_g and μ_g being the geometric standard deviation and geometric mean respectively, and θ , the offset value.

The gamma distribution yields more accurate rainfall rate computations than the exponential distribution, especially when combined with radar data [13]. The gamma distribution is given as

$$N(D) = N_T D^\mu \exp(-\Lambda D), \quad 0 \leq D \leq D_{max} \tag{4}$$

with Λ, μ , and N_T as the slope, shape and scaling parameters respectively, and these allow for the characterisation of a wide range of rainfall scenarios. The exponential distribution is a special case of the gamma distribution with $\mu = 0$.

However, these distributions do not describe all DSDs, as it has been suggested that different rain types [14, 15] and regions [13, 16, 17] may be described by different statistical models. Previous works [5–7, 18–20] present cases where these unimodal distributions do not adequately describe distributions that are distributed multimodally. Ekerete, *et al.* [6] proposes that these distributions be modelled with a Gaussian Mixture Model (GMM) in the log domain.

The GMM probability density function is given as [7]

$$p(D) = \sum_{i=1}^k w_i \cdot \frac{1}{D} \exp \left[-\frac{(\ln(D) - \mu_i)^2}{2\sigma_i^2} \right] \tag{5}$$

where μ_i and σ_i are the mean and standard deviation of the i^{th} mode respectively and the weights w_i have the property $\sum_{i=1}^k w_i = 1$.

3 Attenuation Due to Rain

3.1 Specific Attenuation

Radio signals travelling through the earth-space paths are attenuated, the severity depending on many factors; frequency, temperature, pressure, as well as the presence of precipitation, chiefly raindrops. The higher the frequency, the higher the signal impairment as the wavelength to raindrop diameter ratio becomes smaller.

Specific rain attenuation, measured in dB/km, is the attenuation of the signal due to rain per unit distance. At any given point in the earth-space path, the specific attenuation is largely dependent on the rain rate at that point. Integrating the specific attenuation along the path gives the total attenuation [21]. The specific attenuation can be estimated by assuming spherical raindrops and using Mie's scattering theory [22].

The received power, P_r , on a uniformly distributed spherical water drop of radius r with transmitted power, P_t , over length L is given as

$$P_r = P_t \cdot \exp(-kL) \quad (6)$$

where k is the attenuation coefficient for the rain volume expressed in units of reciprocal length.

The attenuation, A (in dB) will be given as

$$A = 10 \cdot \log_{10}(P_t/P_r) = 10 \cdot \log_{10} \exp(kL) = 4.343 \cdot kL \quad (7)$$

where the attenuation coefficient, k , is

$$k = N(D) \cdot Q_t \quad (8)$$

and $N(D)$ is the drop density, and Q_t is the extinction cross section of the drop with diameter D [23].

An alternative approach to estimating the specific attenuation is given by the ITU-R P.838-3 [24], where the specific attenuation, γ in (dB/km), is given as a power law relationship dependent on the rain rate, R .

$$\gamma = a \cdot R^b \quad (9)$$

where the coefficients a and b are dependent on the frequency, f (GHz), and given in [24].

3.2 Extinction Cross Section

The extinction (or attenuation) cross section, Q_t , is dependent on the wavelength, λ , the complex refractive index of water, $m = p + iq$ and the drop diameter, D . $Q_t = Q_t(\lambda, m, D)$. A deeper treatment of the extinction cross section is given by [25].

The attenuation coefficient is determined by integration over all the drop sizes since the drop sizes are not all equal, the attenuation coefficient is given as

$$k = \int_0^\infty Q_t(\lambda, m, D) N(D) dD \tag{10}$$

The specific attenuation is then given as [14]

$$\gamma = 4.343 \int_0^\infty Q_t(\lambda, m, D) N(D) dD \text{ dB/km} \tag{11}$$

According to Mie’s theory for a plane wave radiation on an absorbing sphere, the wave number $x = \pi D/\lambda$.

The complex forward scattering amplitude for the spherical raindrop function is given as [26]

$$S(0) = \frac{1}{2} \sum_{n=1}^\infty (2n + 1)(a_n + b_n) \tag{12}$$

This gives the extinction cross section as

$$Q_t = \frac{4\pi}{k^2} Re S(0) = \frac{2}{x^2} \sum_{n=1}^\infty (2n + 1) Re(a_n + b_n) \tag{13}$$

where a_n and b_n are the Mie scattering coefficients, complex functions of λ , m and D .

3.3 How Specific Attenuation Scales with Drop Size

It is interesting to see how the ITU specific attenuation scales theoretically as drop size varies, whilst keeping rain rate constant. To do this, it is assumed the drops are all identically sized spheres of diameter D . Then the number of drops falling on a plane surface at a constant rain rate R scales proportional to D^{-3} . The specific attenuation depends on the spatial distribution of drops in the atmosphere, which is the number of drops per unit volume. This depends on the fall speed of drops. A common approximation to this is that the terminal velocity of drop is proportional to $D^{0.67}$ [27]. Thus the number of rain drops per unit volume scales as $D^{-3.67}$. Mie scattering theory says that the specific attenuation is proportional to the number of drops multiplied by the extinction cross section Q_t . At 20 GHz, Q_t can be approximated as proportional to D^4 [28]. Hence the specific attenuation at constant rain rate scales approximately as $D^{1/3}$, i.e. attenuation at constant R increases with drop size. This suggests that the attenuation predicted by the ITU-R model, which is of the form kR^α (for constants k and α), will be high for small drop sizes and low for large drop sizes.

4 Data and Procedures Used in the Study

4.1 Data Collection and Processing

Data from the Chilbolton Observatory (51.14° N, 1.44° W) were collected and analysed. This data is from a RD69 JWD impact disdrometer, and a co-located rain gauge’s data from 2010 to 2013.

The JWD impact disdrometer, with a sampling cross-sectional area of 50 cm² measures the size of raindrops falling on its top Styrofoam® cup by converting the impact into electrical pulses, and the amplitude of the impulse is then used to determine the diameter of the drops. The measurements are sorted into 127 increasingly non-uniform groupings termed channels or bins depending on the amplitude of the impacting rainfall. Algorithms convert the recorded amplitude to drop diameters. This is accurate to ±5% [29].

The disdrometer and the rain gauge collects data at 10 s interval, but this study merges this into 1 min samples with the assumption that the underlying distribution does not change radically over the 1 min period considered. This study only considered rain events with rates greater than 0.1 mm/h.

The drop velocities for rain with diameter D_i , was taken to be [30]:

$$v_i = 9.65 - 10.3 \cdot \exp(-0.6D_i) \tag{14}$$

The rain rate (in mm/h) at time instant t , (in seconds) was derived as:

$$R_t = \frac{3600 \cdot \sum V_i \cdot n_i(t)}{\Delta t \cdot A} \tag{15}$$

where V_i is the drop volume, n_i is the drop counts, Δt is the integration time and A is the disdrometers’s cross section.

The parameters for the disdrometer at Chilbolton are as follows (Table 1):

Table 1. Parameters for the disdrometer at Chilbolton Observatory for ITU-R P.838

Parameter	Value
Latitude	51.14°N
Longitude	357.74°E
Frequency	19.7 GHz
Elevation angle	29.9°
Tilt angle	13°
Height above sea level	84 m

Given the above, the a and b , as derived from the suggestions of ITU-R P.838-3 are 0.0907 and 1.0229 respectively.

4.2 Procedures

Six consecutive 10 s samples were merged. This was done to achieve a larger sample size, with the implicit assumption that the underlying distribution is approximately stationary over the one minute period under consideration. This is similar to the approaches adopted by Montopoli *et al.* [31], Townsend *et al.* [32] and Islam *et al.* [33].

Given the doubt about the reliability of the smaller drops measurements [1, 34, 35], especially in the JWD, this work considered only bins with drop diameters greater 0.6 mm. This consideration resulted in a sample of 93 super bins, with the boundaries determined by the ETH re-calibration given in McFarquhar and List [36].

Based on the rain rates computed from Eq. (16) and the k and α determined, the specific attenuation based on the ITU-R P. 838-3 recommendation was computed using the relationship $\gamma = a R^b$ (Eq. 9).

The method of Mätzler [37] was used to determine the extinction cross section, Q_r , from the Mie's coefficients at 19.7 GHz (the radio wave frequency), with the refractive index of water taken as $m = 6.867 + 2.630i$ [38].

For each 1 min sample above the rainfall threshold, (taken here to be 0.1 mm/h), the DSD was computed from the disdrometer's rain drop counts, and each was compared to a co-located rain gauge to ensure accuracy.

The lognormal and gamma (using the method of moments, MoM) were fitted to the 1 min spatial drop density data. Equally, the GMM, using the number of modes specified in Ekerete *et al.* [6] were fitted for the observed number of modes.

For each of these distributions (spatial drop densities, lognormal, gamma (MoM), and the GMMs based on the observed number of modes), the specific attenuation were computed for each one minute sample, showing how each drop diameter volume affects the signals. The results were compared with that derived from the ITU-recommended specific attenuation calculations.

5 Results and Interpretations

Based on the methodology described in 4.2 above, the rainfall DSD (shown in the upper panels of Figs. 1 and 2) were used to derive the specific attenuation for a 1-minute time slice. The specific attenuation was derived from the drop densities, shown as bars in the lower panel and the computed specific attenuation for 1st May, 2012 at 0037 and 0053 gave the following:

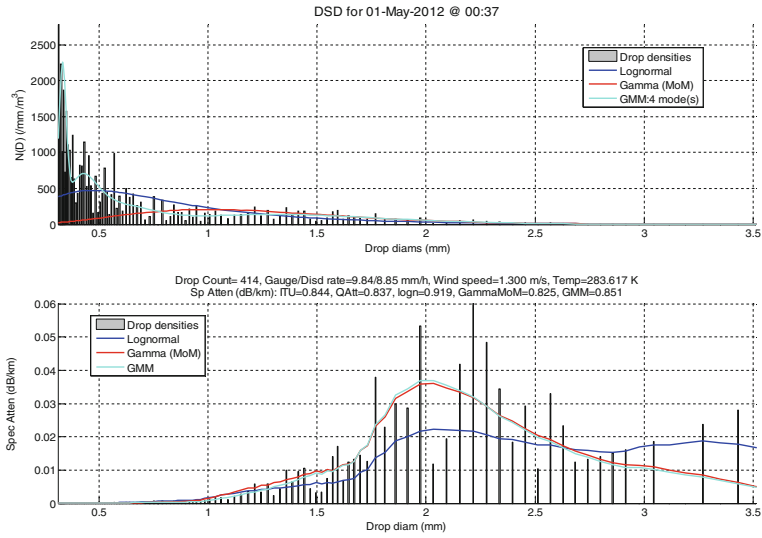


Fig. 1. DSD and specific attenuation, with corresponding meteorological readings for 1-May-2012/0037

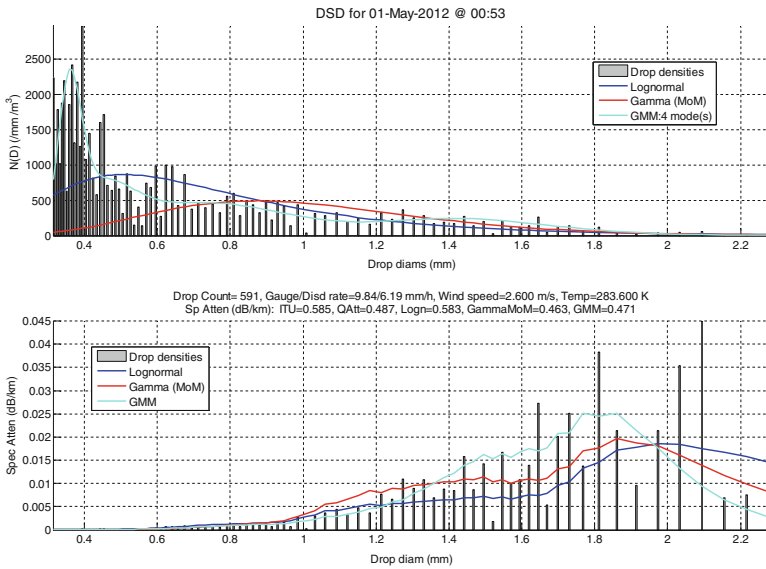


Fig. 2. DSD and specific attenuation, with corresponding meteorological readings for 1-May-2012/0053

Results show that the small-sized drops contribute little to the overall attenuation, as seen by the near flat curve in the graphs. The larger drops contribute more to the

overall attenuation, even when the number of drops are small. This is shown clearly in Fig. 2, where attenuation is high (right side lower panel) even with very few drops.

Using the specific attenuation drawn from the drop densities, it can be seen (from Table 2) that specific attenuation computed from the GMM may be better than those derived from other statistical models. This may be explained from the fact that the GMM models the multimodality present in the data better than the other unimodal distributions.

Table 2. Summary of results for the specific attenuation

Date	01-May-2012	01-May-2012	
Time	00:37	00:53	
Drop count	414	591	
Disdrometer rain rate	8.85	6.19	mm/h
Rain gauge rain rate	9.84	9.84	mm/h
Specific attenuation			
ITU	0.844	0.585	dB/km
Drop density	0.837	0.487	dB/km
Lognormal	0.919	0.583	dB/km
Gamma (MoM)	0.825	0.663	dB/km
GMM	0.851	0.471	dB/km

6 Conclusions

This work has shown that the small drops in the DSD contribute little to the overall attenuation of signals as it passes through the earth-space path. It also demonstrated that larger drops, even in small numbers contribute greatly to the overall attenuation of signals. Results equally suggest that the Gaussian Mixture Model may sometimes model specific attenuation better than unimodal statistical models, as the GMM gives a better fit to multimodality encountered in rainfall DSD data.

While the data set used in this work is small, there is a need to investigate further the seasonal variation of the fit of the attenuation, as well as the variation of the specific attenuation in different rain regimes. The authors are working on realizing the above in the next phase of the research.

References

1. Kumar, L.S., Lee, Y.H., Ong, J.T.: Truncated gamma drop size distribution models for rain attenuation in Singapore. *IEEE Trans. Antennas Propag.* **58**(4), 1325–1335 (2010)
2. Thurai, M., Bringi, V.N., Shimomai, T.: 20 GHz Specific attenuation calculations using drop size distributions and drop shape measurements from 2D video disdrometer data in different rain climates. In: *6th International Conference on Information, Communications & Signal Processing*. IEEE, Singapore (2007)
3. Åsen, W., Gibbins, C.J.: A comparison of rain attenuation and drop size distributions measured in Chilbolton and Singapore. *Radio Sci.* **37**(3), 6-1–6-15 (2002)

4. Ekerete, K.-M.E., Hunt, F.H., Otung, I.E., Jeffery, J.L.: Multimodality in the rainfall drop size distribution in southern England. In: Pillai, P., Hu, Y.F., Otung, I., Giambene, G. (eds.) *WiSATS 2015*. LNICSSITE, vol. 154, pp. 177–184. Springer, Heidelberg (2015). doi: [10.1007/978-3-319-25479-1_13](https://doi.org/10.1007/978-3-319-25479-1_13)
5. Ekerete, K.E., et al.: Experimental study and modelling of rain drop size distribution in southern England. In: *IET Colloquium on Antennas, Wireless and Electromagnetics*, London (2014)
6. Ekerete, K.E., et al.: Variation of multimodality in rainfall drop size distribution with wind speeds and rain rates. *J. Eng.* (2016)
7. Ekerete, K.E., et al.: Modeling rainfall drop size distribution in southern England using a Gaussian Mixture Model. *Radio Sci.* (2015)
8. Marshall, J.S., Palmer, W.M.K.: The distribution of raindrops with size. *J. Meteorol.* **5**(4), 165–166 (1948)
9. Levin, L.M.: The distribution function of cloud and rain drops by sizes. *Dokl. Akad. Nauk SSSR* **94**(6), 1045–1048 (1954)
10. Markowitz, A.H.: Raindrop size distribution expressions. *J. Appl. Meteorol.* **15**(9), 1029–1031 (1976)
11. Feingold, G., Levin, Z.: The lognormal fit to raindrop spectra from frontal convective clouds in Israel. *J. Appl. Meteorol.* **25**(10), 1346–1363 (1986)
12. Owolawi, P.: Raindrop size distribution model for the prediction of rain attenuation in Durban. *PIERS Online* **7**(6), 516–523 (2011)
13. Ulbrich, C.W., Atlas, D.: Assessment of the contribution of differential polarization to improved rainfall measurements. *Radio Sci.* **19**(1), 49–57 (1984)
14. Adimula, I.A., Ajayi, G.O.: Variations in raindrop size distribution and specific attenuation due to rain in Nigeria. *Ann. Telecommun.* **51**(1–2), 87–93 (1996)
15. Maitra, A., Chakravarty, K.: Raindrop size distribution measurements and associated rain parameters at a tropical location in the Indian region (2005)
16. Ajayi, G.O., Olsen, R.L.: Modeling of a tropical raindrop size distribution for microwave and millimetre wave applications. *Radio Sci.* **20**(2), 193–202 (1985)
17. Maciel, L.R., Assis, M.S.: Tropical rainfall drop-size distribution. *Int. J. Satell. Commun.* **8**, 181–186 (1990)
18. McFarquhar, G.M.: Raindrop size distribution and evolution. In: *Rainfall: State of the Science*, Geophysical Monograph Series, vol. 191, pp. 49–60 (2010)
19. Radhakrishna, B., Rao, T.N.: Multipeak raindrop size distribution observed by UHF/VHF wind profilers during the passage of a mesoscale convective system. *Mon. Weather Rev.* **137**(3), 976–990 (2009)
20. Sauvageot, H., Koffi, M.: Multimodal raindrop size distribution. *J. Atmos. Sci.* **57**, 2480–2492 (2000)
21. Olsen, R.L., Rogers, D.V., Hodge, D.B.: The aRb relation in the calculation of rain attenuation. *IEEE Trans. Antennas Propag.* **AP-26**(2), 318–329 (1978)
22. Mie, G.: Beiträge zur Optik trüber Medien, speziell kolloidaler Metallösungen. *Ann. Phys.* **330**, 377–445 (1908)
23. Ippolito, L.J.: *Satellite Communications Systems Engineering: Atmospheric Effects, Satellite Link Design and System Performance*. Wiley, Washington, DC (2008)
24. ITU-R: R-REC-P.838-3 - Specific attenuation model for rain for use in prediction methods (2005)
25. Mishchenko, M.I., et al.: On definition and measurement of extinction cross section. *J. Quant. Spectrosc. Radiat. Transfer* **110**, 323–327 (2009)
26. van de Hulst, H.C.: *Light Scattering by Small Particles*. Wiley, New York (1957)

27. Ulbrich, C.W.: Natural variations in the analytical form of the raindrop size distribution. *J. Clim. Appl. Meteorol.* **22**, 1764–1775 (1983)
28. Odedina, M.O., Afullo, T.J.: Determination of rain attenuation from electromagnetic scattering by spherical raindrops: theory and experiment. *Radio Sci.* **45**(1) (2010)
29. Distromet: Disdrometer RD-80, D. Ltd, Editor, Switzerland (2002)
30. Atas, D., Srivastava, R.C., Sekhon, R.S.: Doppler radar characteristics of precipitation at vertical incidence. *Rev. Geophys. Space Phys.* **11**, 1–35 (1973)
31. Montopoli, M., et al., Statistical characterization and modeling of raindrop spectra time series for different climatological regions. *IEEE Trans. Geosci. Remote Sens.* **46**(10) (2008)
32. Townsend, A.J., Watson, R.J.: The linear relationship between attenuation and average rainfall rate for terrestrial links. *IEEE Trans. Antennas Propag.* **59**(3), 994–1002 (2011)
33. Islam, T., et al.: Characteristics of raindrop spectra as normalized gamma distribution from a Joss-Waldvogel disdrometer. *Atmos. Res.* **108**, 57–73 (2012)
34. Thurai, M., et al.: Towards completing the rain drop size distribution spectrum: a case study involving 2D video disdrometer, droplet spectrometer, and polarimetric radar measurements in Greely, Colorado. In: AMS Conference on Radar Meteorology, Norman, Oklahoma, USA (2015)
35. Tokay, A., Kruger, A., Krajewski, W.F.: Comparison of drop size distribution measurements by impact and optical disdrometers. *J. Appl. Meteorol.* **40**, 2083–2097 (2001)
36. McFarquhar, G.M., List, R.: The effect of curve fits for the disdrometer calibration on raindrop spectra, rainfall rate, and radar reflectivity. *J. Appl. Meteorol.* **32**, 774–782 (1993)
37. Mätzler, C.: MATLAB Functions for Mie Scattering and Absorption. Institut für Angewandte Physik (2002)
38. Segelstein, D.: The Complex Refractive Index of Water, University of Missouri, Kansas City, USA (1981)